Fully-coupled 3D Simulation of Electromagnetic Forming*

M. Stiemer[1], J. Unger[2], H. Blum[1], B. Svendsen[2]

[1]Chair of Scientific Computing, University of Dortmund
[2]Chair of Mechanics, University of Dortmund

Abstract

Electromagnetic metal forming is a contact-free high-speed forming process in which strain rates of more than $10^3\ s^{-1}$ are achieved. The deformation of the workpiece is driven by a material body force, the Lorentz force, that results from the interaction of a pulsed magnetic field with eddy currents induced in the workpiece by the magnetic field itself. The purpose of this work is to present a fully-coupled 3D simulation of the process. For the mechanical structure a thermoelastic, viscoplastic, electromagnetic material model is relevant, which is incorporated in a large-deformation dynamic formulation. The evolution of the electromagnetic fields is governed by Maxwell's equations under quasistatic conditions. Their numerical solution in 3D requires particular arrangements due to a reduced regularity at material interfaces. Hence, Nédélec elements are employed. Coupling between the thermomechanical and electromagnetic subsystems takes the form of the Lorentz force, the electromotive intensity, and the current geometry of the workpiece. A staggered scheme based on a Lagrangian mesh for the workpiece and an ALE formulation for the electromagnetic field is utilized to solve the coupled system, guaranteeing the efficiency and accuracy of the data transfer between the two meshes.

Keywords:

Modeling, Viscoplasticity, Electromagnetic metal forming

1 Introduction

Electromagnetic metal forming (EMF) is a contact-free high-speed forming process in which strain rates of more than $10^3\ s^{-1}$ are achieved. In this process, the deformation of the workpiece

This work was carried out in the context of the German Research Foundation (Deutsche Forschungsgemeinschaft (DFG)) Research Group FOR 443. The authors would like to thank the DFG for its financial support.

is driven by a material body force, the Lorentz force, that results from the interaction of a pulsed magnetic field with eddy currents induced in the workpiece by the magnetic field itself. The magnetic field is triggered by a tool coil adjacent to the workpiece, which is excited by the discharging current of a capacitor bank. Fig. 1 displays a typical device for sheet metal forming.

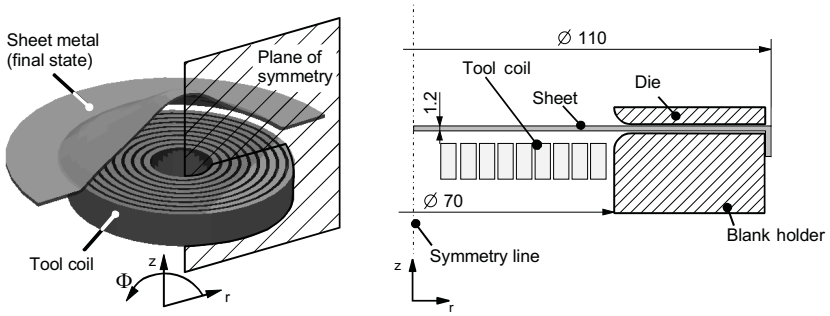

Figure 1: *A typical device for electromagnetic sheet metal forming*

EMF offers certain advantages over other forming methods such as an increased formability, a reduction in wrinkling, reduced tool making costs, the opportunity to combine forming and assembly operations, the avoidance of contact, and many more. However, the highly dynamic nature of this process inhibits its monitoring and control. Consequently, its industrial use has been limited to joining tubular semi-finished materials, while e.g. electromagnetic sheet metal forming is not ready for a profitable application yet. This emphasizes the significance of reliable simulations of this process to identify relevant process parameters and to optimize them.

Since the introduction of high speed computers in the 1980s, several attempts at the numerical simulation of EMF have been undertaken, including [1, 2, 3, 4]. More recently, [5, 6] and [7] utilized commercial programs like ABAQUS or MARC for the simulation of the process. However, in all approaches reported on above emphasis is placed on the modeling and simulation of the coupling between the electromagnetic and the mechanical model, while the employed material models were not adapted to the particular requirements of the process. These include first of all a consideration of the rate-dependence, which is typical of the behavior of metallic materials at high forming rates such as those achieved during EMF. This is connected to the fact that the mechanical dissipation may result in a possibly significant temperature increase in this nearly adiabatic process. A relevant thermodynamically-consistent electromagnetic thermoelastic multifield model has been developed in [8, 9] and implemented in [10], based on a Lagrangian formulation for the mechanical system and an Eulerian formulation on a fixed mesh for the electromagnetic system within an axisymmetric context.

A further drawback of the numerical schemes reported on above is their restriction to two-dimensional or axisymmetric situations. However, practical forming devices often significantly deviate from axisymmetry. Beside the much larger number of unknowns that dramatically increase the numerical expenses necessary to solve the problem and that require much more sophistication to avoid unacceptably long computing times, three-dimensional electromagnetic simulations demand a particular numerical treatment due to the lack of smoothness solutions to Maxwell's equations typically exhibit at material interfaces: A standard approach based on finite elements that enforce continuity of the approximation leads to a poor approximation of the jumps of the normal component of the electromagnetic field at material interfaces. There are several methods to cope with this difficulty, including penalty or least square methods. In this

work, Nédélec elements [11, 12] are applied, which imitate the regularity of the electromagnetic field. Instead of values in the vertices of the cells of the finite elements discretization, integral mean values over the edges represent the degrees of freedom of these elements. Nédélec elements have also been chosen in [13] to simulate three-dimensional coupled electromagnetic mechanical systems, where emphasis is laid on a fast solution of the coupled system via a multigrid solver. However, these results do not apply for EMF since the mechanical system is restricted to linear elasticity. A further difficulty arises from the fact that a Coulomb gauge condition, which is always satisfied in plane or axisymmetric situations, is not automatically fulfilled and has to be cared for. In this work, a novel non-isoparametric version of Nédélec elements is presented working with trial functions with zero divergence such that the Coulomb gauge condition is automatically fulfilled without any further requirements. This simplifies the system equations to be discretized significantly.

There are several coupling mechanisms between the thermomechanical and the electromagnetic subsystem. On the one hand, the Lorentz force computed from the electromagnetic simulation serves as load term in the mechanical impulse balance. On the other hand, the conductivity distribution entering the electromagnetic simulation via the diffusivity is determined by the current position of the structure. Further, the electromotive intensity represents an additional coupling term. The most natural way to discretize the field equations in the context of their usual formulation is to employ a fixed Eulerian mesh for the electromagnetic field and to use a moving Lagrangian mesh for the mechanical structure. However, there are problems inherent to this approach since the character of the electromagnetic field equation in a certain point of the electromagnetic mesh changes from one instant to another when the structure moves over it: As long as it is not covered by the mechanical structure, the field equations are elliptic (instantaneous assumption of the equilibrium field) and they become parabolic (diffusion process) as soon as the point is covered by the structure. This leads to a sudden change in the local discretizations since in the first case there is no explicit dependency on values of the preceding instant, while in the second case there is. Methods that rely on this Euler-Lagrange approach are sometimes called *fictitious boundary method* and are also applied to simulate liquid-structure interaction in computational fluid dynamics (e.g. [14, 15]). They are known to produce bad approximations to the forces exerted on the mechanical structure since oscillations are inevitable as long as the discretization in the (moving) transition zone between the structure and the air is not resolved very finely. However, averaged quantities are quite good approximated with this approach, even with relatively coarse discretizations. In [10], the deformation of the structure could be computed in good accuracy since the determination of the deformation field canonically includes temporal and spatial averaging of the forces applied.

However, if a good approximation to the forces is required an ALE-based method is more promising. Here, the position of the electromagnetic mesh is adapted to the current position of the structure such that the character of the electromagnetic field equations as well as the local discretizations never change. In the approach presented here, this is done in such a way that the combinatorial structure of the mesh can be maintained during the simulation, which allows the use of effective methods like fast multigrid solvers for the solution of the resulting linear system of equations.

2 Coupled model for conducting, thermoelastic viscoplastic metals

The multifield material model applied in this work is derived from a general continuum thermodynamic approach [8, 9] to the formulation of models for electromagnetic thermoelastic solids. For all structural problems of interest the frequencies of relevance (i.e. less than 10 MHz) correspond to electromagnetic wave lengths which are much larger than the structures of interest. Hence, the wave character of the electromagnetic fields is insignificant and can be neglected for such structural problems. This represents the so-called quasistatic approximation [16, §2.2 and §8.2]. In this case, it is shown in [9] that Maxwell's relations together with Ohm's law and the Coulomb gauge condition $\mathrm{div}_{\mathrm{s}}\boldsymbol{a} = 0$ (e.g. [17], §6.5) result in the weak forms*

$$\begin{aligned} \int_R \overset{*}{\boldsymbol{a}} \cdot \boldsymbol{a}_* + \{\zeta\, \boldsymbol{I} + \kappa_{\mathrm{EM}}\, \nabla_{\mathrm{s}}\boldsymbol{a}\} \cdot \nabla_{\mathrm{s}}\boldsymbol{a}_* &= \int_{\partial R} \{\zeta\, \boldsymbol{I} + \kappa_{\mathrm{EM}}\, \nabla_{\mathrm{s}}\boldsymbol{a}\}\boldsymbol{n} \cdot \boldsymbol{a}_* \\ \int_R \nabla_{\mathrm{s}}\chi \cdot \nabla_{\mathrm{s}}\chi_* &= \int_{\partial R} (\nabla_{\mathrm{s}}\chi \cdot \boldsymbol{n})\chi_* \end{aligned} \tag{1}$$

for all test fields $\boldsymbol{a}_*$ and χ_* with respect to a domain R containing the workpiece, the tool coil, and a large area of air around the tool coil and the workpiece. As usual, the test fields vanish on those parts of ∂R where $\boldsymbol{a}$ and χ are specified. Here, χ denotes the electric scalar potential, $\boldsymbol{a}$ the magnetic vector potential, connected to the flux density $\boldsymbol{b}$ via $\boldsymbol{b} = \mathrm{curl}_{\mathrm{s}}\boldsymbol{a}$, $\zeta := \chi - \boldsymbol{a} \cdot \boldsymbol{v}$ a Euclidean frame-indifferent form of the scalar potential, $\boldsymbol{I}$ a second order unit tensor, $\overset{*}{\boldsymbol{a}} := \partial\boldsymbol{a} + (\nabla_{\mathrm{s}}\boldsymbol{a})\boldsymbol{v} + (\nabla_{\mathrm{s}}\boldsymbol{v})^{\mathrm{T}}\boldsymbol{a}$ the objective time-derivative of $\boldsymbol{a}$, and $\kappa_{\mathrm{EM}} = \sigma_{\mathrm{EM}}^{-1}\mu_{\mathrm{EM}}^{-1}$ the magnetic diffusivity computed from the electric conductivity σ_{EM} and the permeability μ_{EM}. For the materials involved ferro-magnetic effects are not relevant and μ_{EM} can be constantly set to the value of the permeability of the vacuum. The conductivity σ_{EM} equals zero outside the tool coil and the workpiece, resulting in an infinite diffusivity there. This means that the equilibrium distribution of the magnetic vector potential depending on its current values on the interface to the tool coil and to the workpiece is instantaneously assumed in each time step. Finally, ∇_{s} represents the usual nabla-operator in the spatial variables. Note that the Coulomb gauge condition does not automatically hold for three-dimensional problems such that it has to be considered explicitly. On the timescale $\tau_{\mathrm{Exp}} \sim 10^{-4}$ s relevant to EMF the typical order of magnitude $\kappa_{\mathrm{EM}} \sim 10^{-1}$ m^2 s^{-1} implies that magnetic diffusion will be important in the process since it takes place over lengthscales of $\sqrt{\kappa_{\mathrm{EM}}\,\tau_{\mathrm{Exp}}} \sim 10$ cm, which are significantly larger than the smallest dimension of interest (e.g. sheet metal thickness ~ 1 mm). Turning next to the mechanical part of the coupled model, the weak momentum balance for the deformation field $\boldsymbol{\xi}$ is given by

$$\int_{B_{\mathrm{r}}} (\varrho_{\mathrm{r}}\, \ddot{\boldsymbol{\xi}} - \boldsymbol{f}) \cdot \boldsymbol{\xi}_* + \boldsymbol{P} \cdot \nabla_{\mathrm{r}}\boldsymbol{\xi}_* = \int_{\partial B_{\mathrm{r}}} |\mathrm{cof}(\boldsymbol{F})\boldsymbol{n}_{\mathrm{r}}|\, \boldsymbol{t}_{\mathrm{c}} \cdot \boldsymbol{\xi}_* \tag{2}$$

with respect to the referential configuration $B_{\mathrm{r}} \subset R$ of the workpiece for all corresponding test fields $\boldsymbol{\xi}_*$ vanishing on those parts of the current boundary ∂B_{c} where $\boldsymbol{\xi}$ is specified. Here, $\boldsymbol{f} = \det(\boldsymbol{F})\, \boldsymbol{j} \times \boldsymbol{b}$ represents the Lorentz (body) force (density), $\boldsymbol{P}$ the first Piola-Kirchhoff stress, $\boldsymbol{F} := \nabla_{\mathrm{r}}\boldsymbol{\xi}$ the deformation gradient, and $\boldsymbol{t}_{\mathrm{c}}$ the current boundary traction. The mechanical model

For notational simplicity the volume dv and surface da elements are dispensed with in the corresponding integrals.

relations are completed by the specification of the material model. For a given thermodynamic state of the mechanical structure $\boldsymbol{P}$ can, as usual, be computed from the free Helmholtz-energy stored in the material. The evolution of its density ψ_{f} is determined by the evolution of certain inner variables, which are in this case the accumulated inelastic strain, the elastic left Cauchy Green tensor, and the temperature. Characteristic for the viscoplastic material model here is a power law approximation to the inelastic potential determining the inelastic part of ψ_{f}. Hence, the projection onto the yield surface typical of rate independent J2-plasticity is replaced by a power-law function, penalizing over-stresses. See [8, 9] for a detailed discussion.

3 An ALE approach to the coupled problem

In the above formulation the mechanical field is given in a Lagrangian formulation, while the electromagnetic field is given in an Eulerian formulation. The most natural discretization of the field equations leads to a moving mesh for the mechanical system, representing its current configuration and a fixed Eulerian mesh for the electromagnetic field. The whole coupled system is then solved via a staggered solution algorithm. However, this approach implicates serious difficulties in the data transfer between the two meshes: In those areas of the electromagnetic mesh currently covered by the moving structure a diffusive process with a positive finite diffusivity takes place, while outside this region the diffusivity is infinite such that the equilibrium state of the field is immediately assumed. As shown in Figure 2, whenever the structure moves those points of the electromagnetic mesh in which a finite diffusivity arises change.

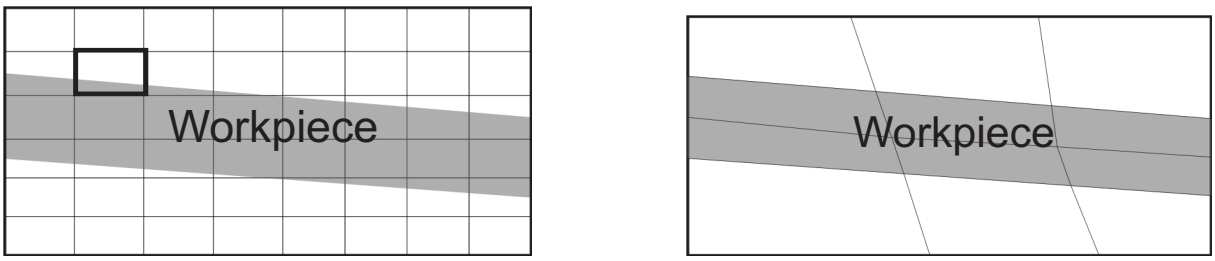

Figure 2: *Comparison of a fictitious boundary method (Euler-Lagrange-approach, on the left) and an ALE-approach (Lagrange-ALE, on the right).*

Such a change alters the local discretization dramatically since a contribution to the mass matrix arises as soon as a point is covered by the structure and it disappears when it is uncovered again. Particularly, for those points of the electromagnetic mesh covered by the mechanical structure values of the last time step are relevant, while the values in the other points do not depend explicitly on those of the preceding time step. It has turned out that this change of the discretization in a certain point of the electromagnetic mesh causes oscillations in the time derivative $\partial \boldsymbol{a}$ of the vector potential and, thus, in the Lorentz force via the contribution $\sigma_{\mathrm{EM}} \partial \boldsymbol{a} \times \mathrm{curl}_{\mathrm{S}}\, \boldsymbol{a}$. These oscillations can be moderated by a very fine discretization of that part of the electromagnetic mesh lying in the interface region of the structure and the surrounding air. To avoid an inadequate fine discretization of the whole structure, adaptive techniques are necessary for a sufficiently fine resolution of the interface region. On the other hand, it is well known that averaged quantities can be determined sufficiently accurate with this approach,

which is sometimes called* *fictitious boundary method*. In [10], it was successfully applied to compute the deformation of a mechanical structure even with relatively coarse discretizations. By the integration of Lorentz forces and due to the time stepping algorithm the above mentioned oscillations are smoothed out. However, as soon as a good and efficient approximation of the forces applied on the mechanical structure is required, a fictitious boundary method is not adequate. In this case, an arbitrary Lagrangian Eulerian (ALE) formulation leads to much better results. In this approach, the electromagnetic mesh is adapted to the moving structure such that always the same elements are covered by the moving mechanical structure (see Fig. 2). Consequently, the character of the discretization in a particular element does never change, which avoids those jumps of $\partial \boldsymbol{a}$ that are typical for the fictitious boundary method. The movement of the electromagnetic mesh is arbitrary in the sense that the position of the discretizing mesh is not determined by requirements of the electromagnetic field equations themselves, but by accompanying conditions. To obtain a high quality mesh for the electromagnetic system with hexahedra elements that deviate as little as possible from the shape of a parallelepiped and that matches the mesh for the mechanical structure, the following algorithm is applied. Before a new time step is started each component of the deformation increment $d\boldsymbol{\xi} = \boldsymbol{\xi}_{n+1} - \boldsymbol{\xi}_n$ is considered as the boundary value of a one-dimensional Dirichlet problem $\Delta u_k = 0$ in the air around tool coil and workpiece (i.e. in those parts of R that are outside the workpiece and outside the tool coil) with boundary values $u_k = d\xi_k$, $k = 1, .., 3$, on the interface between workpiece and air as well as $u_k = 0$ on the interface between tool coil and air and on the *outer boundary* ∂R (i.e. the mesh nodes are held fixed there). The solution of these problems (all possessing the same stiffness matrix) is added to the current positions of the electromagnetic mesh in the air-region around tool coil and workpiece to obtain a mesh for the next time step. To get an impression of the quality of the arising meshes, one can consider the transformation from the old to the new mesh as an elastic deformation with no transversal contraction and with elasticity module 1. This deformation is conducted by the boundary values on the interface to the tool coil, on the workpiece, and on the outer boundary since no forces are assumed to be present. In contrast to remeshing strategies, this approach preserves the combinatorial structure of the mesh, which allows an effective solution of the arising huge systems of linear equations.

The discrete field equations on the electromagnetic mesh have to be reformulated such that the movement of the mesh is correctly considered. Surprisingly, the resulting field equations simplify. Instead of working with the partial time derivative $\partial \boldsymbol{a}$, it is convenient in this case to employ the material time derivative $\dot{\boldsymbol{a}} = \partial \boldsymbol{a} + (\nabla_{\mathrm{s}} \boldsymbol{a})\boldsymbol{v}$ since its discretization is a function of the vertices of the moving mesh inside the mechanical structure rather than of spatial points. Thus, no interpolation is necessary to link past data to current data. Inside the fixed tool coil $\dot{\boldsymbol{a}} = \partial \boldsymbol{a}$ applies and in the air surrounding the tool coil and the workpiece the field assumes an equilibrium position instantaneously, which is explicitly neither depending on values of $\partial \boldsymbol{a}$ nor on values of $\boldsymbol{a}$ from a preceding time step. The weak form for the electromagnetic problem – still under the assumption that a Coulomb gauge is provided for (see the next section) – then

The approaches discussed here are also used to simulate fluid-structure interaction in computational fluid dynamics.

takes the form

$$\begin{aligned} &\int_R \kappa_{\mathrm{EM}}^{-1} \{\dot{\boldsymbol{a}} + \nabla_{\mathrm{s}}\chi - (\nabla_{\mathrm{s}}\boldsymbol{a})^{\mathrm{T}}\boldsymbol{v}\} \cdot \boldsymbol{a}_* + \nabla_{\mathrm{s}}\boldsymbol{a} \cdot \nabla_{\mathrm{s}}\boldsymbol{a}_* = 0 \ , \\ &\int_R \nabla_{\mathrm{s}}\chi \cdot \nabla_{\mathrm{s}}\chi_* = 0 \ , \end{aligned} \tag{3}$$

with the additional approximation $\boldsymbol{a} = \boldsymbol{0}$ and $\chi = 0$ on ∂R, which has been chosen to be a large box containing the tool coil, the workpiece, and a large area of air surrounding them. This approximation is well founded due to the asymptotic decay of the vector and of the scalar potential of a dipole field like $O(|x|^{-2})$, $|x| \to \infty$. At interfaces between different materials further transition conditions have to be considered (see e.g. [13]).

4 Divergence-free discretization of the electromagnetic system

Next, the weak form for the electromagnetic system and for the mechanical system have to be spatially discretized. In the context of the finite-element method, standard eight-node elements are used in the latter case, while Nédélec elements [11, 12] are employed for the vector potential equation in the first case. Nédélec elements represent one of several methods to overcome the problem that finite elements enforcing continuity, as standard nodal finite elements, provide a very poor approximation to $\boldsymbol{a}$ at material interfaces where the normal components of this field possess discontinuities. Moreover, a new non-isoparametric divergence-free use of Nédélec's elements has been developed here that guarantees a Coloumb gauge condition without any further requirements.

The discretization of the Lagrangian formulation of the mechanical system is based, as usual, on a spatial discretization of the mechanical structure with eight-node brick elements, each of which is the image of a reference cube under transformations that form an isoparametric family. All integrations necessary to compute the local contributions of these elements to the stiffness matrix are pulled back to the referential cube. The same strategy is applied to solve the equation for the electro-magnetic scalar potential. In case of the vector potential equation, however, no transformation on a referential cube is performed, but in each element of the discretization $R \approx \bigcup_e R^e$ of R into a finite number of hexahedra R^e a local basis of the test and trial space is constructed as follows: To each edge Γ_i of a hexahedron R^e, $1 \leq i \leq 12$, a basis function b_k of the form

$$b_k(x) = \begin{pmatrix} a_{11}^{(k)} & + & a_{12}^{(k)} x_2 & + & a_{13}^{(k)} x_3 & + & a_{14}^{(k)} x_2 x_3 \\ a_{21}^{(k)} x_1 & + & a_{22}^{(k)} & + & a_{23}^{(k)} x_3 & + & a_{24}^{(k)} x_1 x_3 \\ a_{31}^{(k)} x_1 & + & a_{32}^{(k)} x_2 & + & a_{33}^{(k)} & + & a_{34}^{(k)} x_1 x_2 \end{pmatrix} \tag{4}$$

is assigned with

$$\int_{\Gamma_i} b_k \cdot t_i = \delta_{ki} \ , \tag{5}$$

where t_i represents a tangential vector to Γ_i of unit length and δ_{ki} is defined by $\delta_{ii} = 1$, $1 \leq i \leq 12$, and $\delta_{ki} = 0$ for $k \neq i$ respectively. Algorithmically, the determination of the b_k leads to the solution of 12 systems, each of which consists of 12 equations, in any element R^e of the

finite-element discretization. The necessary numerical efforts remain acceptably small since all 12 systems to be solved in a certain element possess the same system matrix and, e.g. MATLAB, solves 100,000 sets of 12 systems of this type within a CPU time of 5.36 s on a 2394 Mhz Opteron machine.

One easily deduces that all b_k are divergence-free and such is the local approximation to the electromagnetic field being a linear combination of these basis functions. The method presented here deviates from the usual employment of Nédélec elements (of first order) where a local basis obeying the above approach (4) is only constructed for a referential cube and then transformed by a family of isoparametric transformations on the *physical* elements such that integrals over the edges of the form (5) remain invariant. However, the local test and trial spaces obtained from this process are no longer divergence-free such that the Coulomb gauge condition is not satisfied. Hence, the weak forms for the scalar and for the vector potential to be discretized contain further terms and are more complicated. Another drawback of an isoparametric family of Nédélec elements results from further approximations that are usually undertaken in the practical implementation of the method: Certain second order terms that are dropped may become significantly large when the shape of the elements deviates too much from a parallelepiped, which may happen, if large deformations occur in the ALE context.

With the shape function matrix $\mathbf{N} \in \mathbb{R}^{12\times 12}$ at hand constructed in the usual fashion from the basis functions b_k, one obtains

$$\boldsymbol{a}_e = \mathbf{N}\mathbf{a}^e$$

for the vector potential field at the element level $\boldsymbol{a}_e$. Here, $\mathbf{a}^e \in \mathbb{R}^{12}$ represents the vector of integral means (5) over the edges of R^e. This implies

$$\nabla_{\mathsf{S}}^e \boldsymbol{a}_e = (\nabla_{\mathsf{S}}^e \mathbf{N})^{\mathsf{S}} \mathbf{a}^e$$

for the corresponding gradient. On this basis, one obtains the spatially-discretized form

$$\mathbf{A}^s\,\mathbf{a}^s + \kappa_{\mathsf{EM}}^{-1}\,\mathbf{B}^s\,\dot{\mathbf{a}}^s = \mathbf{c}^s \tag{6}$$

for the vector $\mathbf{a}^s$ of time-dependent integral means of the form (5) over all edges of the discretization of R. The stiffness matrix $\mathbf{A}^s$, the mass matrix $\mathbf{B}^s$, and the source vector $\mathbf{c}^s$ are assembled from the local contributions

$$\mathbf{A}^e \quad := \quad \int_{R^e} (\nabla_{\mathsf{S}}^e \mathbf{N})^{\mathsf{ST}} (\nabla_{\mathsf{S}}^e \mathbf{N})^{\mathsf{S}} \,,$$

$$\mathbf{B}^e \quad := \quad \int_{R^e \cap W} \mathbf{N}^{\mathsf{T}} \mathbf{N} \,,$$

and

$$\mathbf{c}^e \;:= \int_{R^e \cap W} \mathbf{N}^{\mathsf{T}} \nabla_{\mathsf{S}} \chi$$

of the single elements as usual. The entries of the source vector are computed from the solution χ of the electro-static equation. For simplicity, it has not been indicated in the notation that only a finite-element approximation to χ is available. According to the degenerate parabolic character of the underlying boundary value problem, equation (6) represents an ordinary differential-algebraic system of equations, yielding a purely algebraic relation for those degrees of freedom

lying in the area of infinite diffusivity.

For the simulation of the transient process time stepping algorithms have to be chosen. To solve the dynamic second order equation for the mechanical system, Newmark's method is employed. For the degenerate parabolic electromagnetic equations the generalized trapezoidal rule is utilized. With optimal parameters both methods provide an accuracy of $O(\Delta t^2)$, $\Delta t \to 0$, where Δt denotes the size of the time step.

The coupling may be realized explicitly or implicitly. In an explicit coupling scheme the electromagnetic field of the $(n+1)$th time step is computed from the position of the structure in the nth time step and the position of the structure in the $(n+1)$th time step is then computed according to this field distribution. Hence, in any time step the electromagnetic and the deformation field are only computed once. In an implicit scheme, however, the electromagnetic field is several times recalculated in each time step according to the position of the altered structure and the structure is altered several times according to the changed electromagnetic field. The latter method is more stable and allows for larger time steps. However, if the numbers of unknowns is large an explicit method may be more efficient.

5 Conclusions

A fully-coupled three-dimensional simulation of EMF has been presented based on a thermoelastic, viscoplastic, electromagnetic material model incorporated in a large-deformation dynamic Lagrangian formulation and Maxwell's equations under quasistatic conditions. To compute the applied Lorentz forces in high accuracy, an ALE approach for the electromagnetic fields has been chosen. The adaption of the electromagnetic mesh to the moving structure avoids, on the one hand, unphysical oscillations of the computed forces and simplifies, on the other hand, the field equations. In contrast to remeshing strategies this approach preserves the combinatorial structure of the mesh, which allows an effective solution of the arising huge systems of linear equations. To discretize the electromagnetic system, a novel, non-isoparametric version of Nédélec elements is employed. This formulation guarantees a Coulomb gauge, which simplifies the field relations, avoids a bad approximation at material interfaces due to the discontinuity of the normal component of the vector potential, and, finally, avoids further deviations in case of large mesh deformation, which would arise in an isoparametric context. A comparison of simulations based on the methods presented here to experimental data represents work in progress.

References

[1] *Gourdin, W. H.*: Analysis and assessment of electromagnetic ring expansion as a high-strain rate test. J. Appl. Phys., volume 65: p. 411, 1989.

[2] *Gourdin, W. H.*; *Weinland, S. L.*; and *Boling, R. M.*: Development of the electromagnetically-launched expanding ring as a high strain-rate test. Rev. Sci. Instrum., volume 60: p. 427, 1989.

[3] *Takata, N.*; *Kato, M.*; *Sato, K.*; and *Tobe, T.*: High-speed forming of metal sheets by

electromagnetic forces. Japan Soc. Mech. Eng. Int. J., volume 31: p. 142, 1988.

[4] *Fenton, G.* and *Daehn, G. S.*: Modeling of electromagnetically formed sheet metal. J. Mat. Process. Tech., volume 75: pp. 6–16, 1998.

[5] *Beerwald, C.*; *Brosius, A.*; *Homberg, W.*; *Kleiner, M.*; and *Wellendorf, A.*: New aspects of electromagnetic forming. In *Proceedings of the 6th International Conference on the Technology of Plasticity*, volume III, pp. 2471–2476. 1999.

[6] *Beerwald, C.*; *Brosius, A.*; and *Kleiner, M.*: Determination of flow stress at very high strain-rates by a combination of magnetic forming and FEM calculation. In *Proceedings of the International Workshop on Friction and Flow Stress in Cutting and Forming (CIRP)*. ENSAM - Paris, 2000.

[7] *Brosius, A.*; *Chanda, T.*; *Kleiner, M.*; and *Svendsen, T.*: Finite-element modeling and simulation of material behavior during electromagnetic metal forming. In *Proceedings of the 6th International ESAFORM Conference on Material Forming 28.-30. April 2003, Italy*, pp. 971–974. ESAFORM 2003, 2003.

[8] *Svendsen, B.* and *Chanda, T.*: Continuum thermodynamic modeling and simulation of electromagnetic forming. Technische Mechanik, volume 23: pp. 103–112, 2003.

[9] *Svendsen, B.* and *Chanda, T.*: Continuum thermodynamic formulation of models for electromagnetic thermoinlastic materials with application to electromagnetic metal forming. Cont. Mech. Thermodyn., volume 17: pp. 1–16, 2005.

[10] *Stiemer, M.*; *Unger, J.*; *Blum, H.*; and *Svendsen, B.*: Algorithmic formulation and numerical implementation of coupled multifield models for electromagnetic metal forming simulations. Int. J. Numerical Methods in Engineering, 2006. Accepted.

[11] *Nédélec, J. C.*: Mixed Finite Elements in $\mathbb{R}^3$. Numerische Mathematik, volume 35: pp. 315–341, 1980.

[12] *Nédélec, J. C.*: A New Family of Mixed Finite Elements in $\mathbb{R}^3$. Numerische Mathematik, volume 50: pp. 57–81, 1986.

[13] *Schinnerl, M.*; *Schöberl, J.*; *Kaltenbacher, M.*; and *Lerch, R.*: Multigrid Methods for the 3D Simulation of Nonlinear Magneto-Mechanical Systems. IEEE transactions magnetics, volume 38: pp. 1497–1511, 2002.

[14] *Wan* and *Turek, S.*: Numerical Simulation of Coupled Fluid–Solid Systems by Fictitious Boundary and Grid Deformation Methods. Technical report, FB Mathematik, Universität Dortmund, 2005. Ergebnisberichte des Instituts für Angewandte Mathematik, 305.

[15] *Wan, D.* and *Turek, S.*: Fictitious Boundary and Moving Mesh Methods for the Numerical Simulation of Rigid Particulate Flows. Technical report, FB Mathematik, Universität Dortmund, 2006. Ergebnisberichte des Instituts für Angewandte Mathematik, 310.

[16] *Moon, F.*: *Magnetic interactions in solids*. Springer-Verlag, 1980.

[17] *Jackson, J. D.*: *Classical Electrodynamics*. John Wiley and Sons, 1987.